Scientific Research Publishing

Open Journal of Inorganic Chemistry, 2023, 13, 1-24
https://www.scirp.org/journal/ojic
ISSN Online: 2161-7414
ISSN Print: 2161-7406

Effect of Changing Anion on the Crystalline Structure, Crystal Structure, Hirschfield Surface, IR and NMR Spectroscopy of Organic Salts and Hybrid Compounds: $C_6H_4(NH_3)_2Cl_2$ (I), β-$[C_6H_{10}N_2]_2ZnCl_4$ (II), Respectively

Nejeh Hannachi[1], Rim Elwej[2*], Thierry Roisnel[3], Faouzi Hlel[1]

[1]Laboratory of Spectroscopic Characterization and Optics of Materials, Faculty of Sciences, University of Sfax, Sfax, Tunisia
[2]National Center for Research in Materials Science (CNRSM), Laboratory for the Valorization of Useful Materials (LVMU), Borj Cedria, Tunisia
[3]CNRS, ISCR (Institute of Chemical Sciences of Rennes), Université de Rennes, Rennes, France
Email: *elwejrim@yahoo.fr

How to cite this paper: Hannachi, N., Elwej, R., Roisnel, T. and Hlel, F. (2023) Effect of Changing Anion on the Crystalline Structure, Crystal Structure, Hirschfield Surface, IR and NMR Spectroscopy of Organic Salts and Hybrid Compounds: $C_6H_4(NH_3)_2Cl_2$ (I), β-$[C_6H_{10}N_2]_2ZnCl_4$ (II), Respectively. *Open Journal of Inorganic Chemistry*, **13**, 1-24.
https://doi.org/10.4236/ojic.2023.131001

Received: November 24, 2022
Accepted: January 25, 2023
Published: January 28, 2023

Abstract

Two organic-inorganic hybrid materials, $C_6H_4(NH_3)_2{\cdot}Cl_2$ (**I**) and β-$[C_6H_{10}N_2]_2ZnCl_4$ (**II**), have been synthesized by hydrothermal method. These two materials are one of the hybrid materials have emerged as one of the most brilliant components classes. These extraordinary compounds synergistically combine the desired physical properties of both organic and inorganic components into a single compound offering the possibility to achieve great improvement over time in terms of science across various sectors. Their structures were determined by XRD pattern investigations and single crystal X-ray diffraction. These two compounds are crystallized in the monoclinic system; $C2/c$ space group. In the both structures, the anionic-cationic entities are interconnected by hydrogen bonding contacts and p-p Interaction forming three-dimensional networks. Intermolecular interactions were investigated by Hirshfeld surfaces and the contacts of the four different chloride atoms in (**II**) were compared. The vibrational absorption bands were identified by infrared spectroscopy. These compounds were also investigated by solid state ^{13}C NMR spectroscopy.

Keywords

Crystal Structure, Hirshfeld Surface, ^{13}C NMR-MAS, Vibration Absorption

1. Introduction

Organic-inorganic metal halides have captivated vigorous concern in the last decades due to both technological features as well as potential applications in several physical properties [1] [2] [3] [4].

The development of new functional materials in particular the hybrid materials has received considerable attention due to their potential application relative to the properties of the as possible interactions connecting of the organic and inorganic species that show weak interactions between the two phases, such as Van Der-Walls, hydrogen bonding or weak electrostatic interactions [5]. In addition, the hybrid compounds represented a stimulus materials science research owing to their myriad characteristics with potential phase transition materials and lightness [6] [7] [8]. Despite the difficulty in predicting the magnetic properties of hybrid materials, recent years have witnessed a renewed interest in the design of magnetic layered organic-inorganic components [9]. The ability of managing the assembling of an extensive variety of structurally well-defined nanoobjects into complex hybrid architectures arranged in a hierarchical order is organized with regard to their structures and functions [10] [11].

Nitrogen containing organic species, which may be aliphatic or aromatic amines [12] [13], are good candidates for synthesis due to their ability to form covalent or iono-covalent bonds with the metallic anions suchas Cd, Zn, Cu… [14] [15] [16]. Hydroxyl and nitrogen containing linkers exhibit a versatile coordination behavior displaying distinct bonding modes toward metal anions [17] [18]. Zinc is one of the most abundant metals in the human body, and it plays an important and indispensable role in biological systems [19]. In addition, the basic zinc hybrids have proved physical properties [20] [21] etc. Also, the zinc complexes exhibit a wide range of coordination numbers and geometries; tetrahedral [22] [23], trigonal bipyramidal [24], and octahedral [25] [26] [27] [28].

Notably, a great process is made using metal-halide compounds, including 1,2-diaminobenzene. For reason of pervasive biological occurrence, performed to the stabilization of compounds [29] [30] [31] [32] hydrogen bonds of hybrid compounds occupy a great interest. The supramolecular networks become specifically interesting when the cation and anion can participate in hydrogen-bonding. Over the past few years, a significant attention has been dedicated to the study of chlorate and nitrate salts containing organic cations thanks to their captivating properties such as ferroelectric and dielectric behaviors [33] [34] [35].

In addition, to the study of this compound family, we focus in this work on the synthesis and the crystal structure of the title compound $C_6H_4(NH_3)_2{\cdot}Cl_2$ (**I**). On a second part, 1,2-diaminobenzene was protonated and combined with metal halides zincate, forming a new hybrid compound β-$[C_6H_{10}N_2]_2ZnCl_4$ (**II**). XRD pattern investigations, single crystal X-ray diffraction, Hirshfeld surface; ^{13}C CP-MAS NMR and vibration absorption for the purpose of confirming its purity and investigating the structural properties marked the compounds' synthesis.

2. Experimental

2.1. Chemical Preparation

The synthesis of the single crystal of $C_6H_4(NH_3)_2{\cdot}Cl_2$ (**I**) and β-$[C_6H_{10}N_2]_2ZnCl_4$ (**II**) compounds was carried out at home-built Teflon-lined stainless steel pressure bombs of 90 ml maximum capacity as follow: 1,2-benzen diammonium $C_6H_8N_2$ (sigma aldrich) was dissolved in a mixture of distilled water (10 mL) and Hydrochloric acid (0.5 mL) (sigma aldrich) for a few minutes with agitation successive to ensure complete dissolution. Second, such solutions were slowly combined in an autoclave and kept at 95˚C under auto-genous pressure for 24 h. After cooling these solutions for five days at room temperature, colourless single crystals $C_6H_4(NH_3)_2{\cdot}Cl_2$ (**I**) suitable for an X-ray structure.

-1, 2-benzen diammonium $C_6H_8N_2$ (0.0801 g; 0.622 mmoles) and Zinc chloride $ZnCl_2$ (0.5032 g; 1.88 mmoles) (sigma aldrich) were dissolved in aqueous solution of HCl (1 M; 37%) for a few minutes with agitation successive to ensure complete dissolution of the compound hydrochloric acid (pH ≈ 1.8). The mixture was placed in a Teflon-lined autoclave that was then sealed and heated to 95˚C for 24 h. It was then allowed to cool to room temperature in a cold water bath. Autoclaves were opened in the air, and products were recovered through filtration. White stick-shaped crystals β-$[C_6H_{10}N_2]_2ZnCl_4$ (**II**) with suitable dimensions for crystallographic study were recovered (Scheme 1).

Schematically the reaction is shown in the following equation.

2.2. Experimental Procedure

- **XRD measurement**

Phase purity and homogeneity of synthesized of both compounds were determined by x-ray powder diffraction recorded at room temperature in the angular range $5^\circ < 2\theta < 80^\circ$ (Figure 1) with a step $\Delta(2\theta) = (0.0170)^\circ$ using a X'Pert PROMPD diffractometer with CuKα1 radiation (λKα1 = 1.540598 Å).

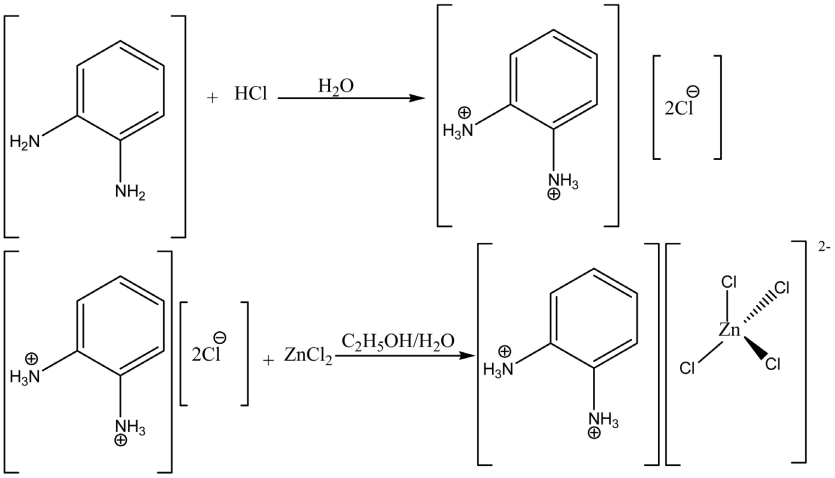

Scheme 1. Synthesis of complexes $C_6H_4(NH_3)_2Cl_2$ (**I**) and β-$[C_6H_{10}N_2]_2ZnCl_4$(**II**), respectively.

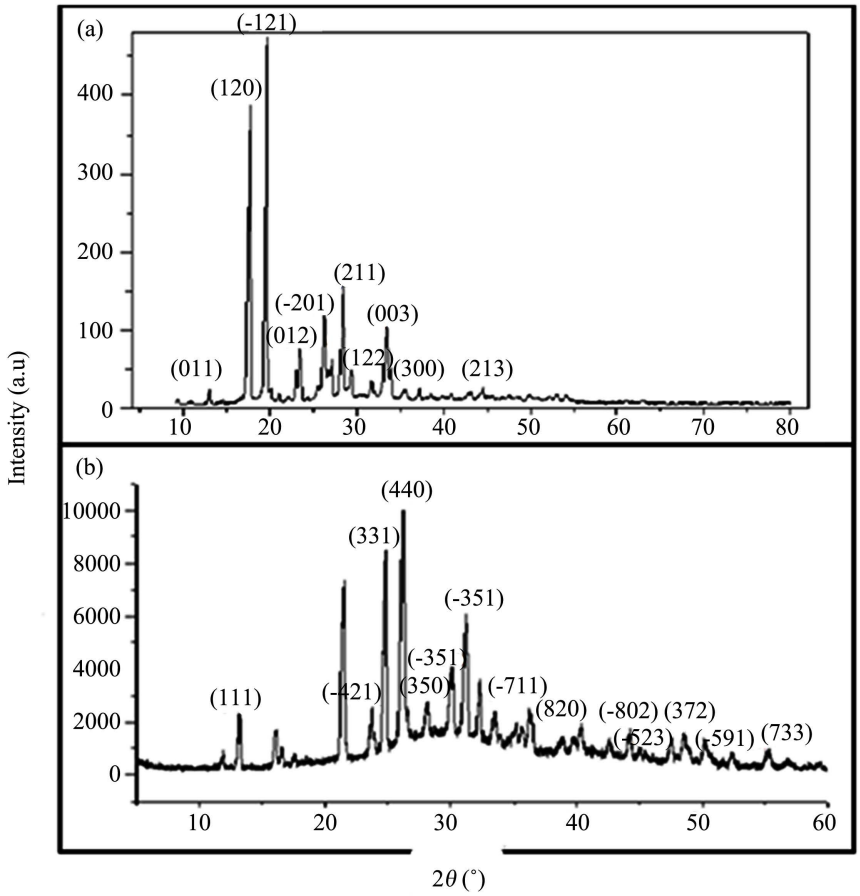

Figure 1. X-ray Powder diffraction patterns of: (a) $C_6H_4(NH_3)_2{\cdot}Cl_2$ (I) and (b) β-$[C_6H_9N_2]_2ZnCl_4$ (II) at room temperature.

- **Single-crystal data collection and structure determination**

Suitable crystals selected through an optical examination were mounted a intensity data were obtained on a D8 VENTURE Bruker AXS diffractometer equipped with a (CMOS) PHOTON 100 detector using Mo K_α radiation (λ = *0.71073* Å, multilayer monochromator) through the Bruker AXS APEX2 Software Suite [36].

Frame integration and data reduction were carried out with the program SAINT [37]. The program SADABS [38] was then employed for multiscan-type absorption corrections. The crystal structure was solved in the monoclinic symmetry, space group C2/c; of two compounds, respectively; according to the automated search for space group available in Wingx [39].

Zinc and chloride atoms were located using the direct methods with the program SIR-2014 [40]. C and N atoms from the amine were found from successive difference Fourier calculations using SHELXL-2014 [41]. Their positions were validated from geometrical considerations as well as from the examination of possible hydrogen bonds. H atoms were positioned geometrically and allowed to ride on their parent atoms. Structural drawings have been made by Diamond 2 [42] program. Crystallographic data are given in **Table 1**.

Table 1. Summary of crystal data and structure refinement.

Complex Empirical formula	$C_6H_4(NH_2)_2{\cdot}2HCl$ (**I**)	β-$[C_6H_{10}N_2]_2ZnCl_4$ (**II**)
Formula weight ($g{\cdot}mol^{-1}$)	181.06	425.47
Crystal system/Space group	Monoclinic, C2/c	Monoclinic, C2/c
Temperature (K)	150	150
Unit cell dimensions		
a (Å)	7.284 (9)	7.443 (3)
b (Å)	14.498 (2)	25.598 (1)
c (Å)	7.945 (1)	9.354 (1)
β (˚)	94.676 (5)	94.017 (2)
V (Å3)/Z	836.4 (2)/4	1777.86 (14)/4
Radiation	Mo Kα	Mo Kα
μ (mm^{-1})	0.703	1.980
h, k, l ranges	$-7 \le h \le 9$ $-18 \le k \le 18$ $-10 \le l \le 10$	$-9 \le h \le 9$ $-33 \le k \le 29$ $-12 \le l \le 12$
Crystal size (mm)	0.58 × 0.51 × 0.35	0.51 × 0.54 × 0.58
Reflections collected/unique/ observed reflections [$I > 2\sigma(I)$]	3745/967/ 930	7007/2003/ 1893
R_{int}	0.0345	0.0259
$(\sin\theta/\lambda)_{max}$ ($Å^{-1}$)	0.649	0.649
Structure refinement with	SHELXL-97	SHELXL-97
Goodness of fit	1.333	1.064
Final R and Rw	0.345/0.0983	0.0259/0.0665
Refinement	F^2 full matrix	F^2 full matrix
Refined parameters	56	67
$\Delta\rho_{max}$, $\Delta\rho_{min}$ (e $Å^{-3}$)	0.8; −0.694 w = 1/[\s^2^(Fo^2^) + (0.0544P)^2^ + 0.3015P] where P = (Fo^2^ + 2Fc^2^)/3	0.743; −0.69 w = 1/[\s^2^(Fo^2^) + (0.0309P)^2^ + 3.1449P] where P = (Fo^2^ + 2Fc^2^)/3

- **Spectroscopy measurements (IR and NMR-MAS)**

The IR absorption spectrum of the crystallized powders in KBr was recorded on a Perkin-Elmer FT-IR 1000 spectrometer in the 400 - 4000 cm^{-1} range. Cross polarization (CP) is to take advantage of the presence of spins abundant (1H) that we will excite to be able to cause a transfer of energy towards the spins scarce (^{13}C). This transfer will be much more effective than just irradiation one

could practice on the small nuclei. The technique cross-polarization (CP) is applied to types of acquisitions. All chemical shifts (d) are given with respect to tetramethylsilane for ^{13}C. According to the IUPAC convention, shielding corresponds to negative values. Spectrum simulation was performed by using Bruker WINFIT software [43].

The NMR-MAS experiments were performed at room temperature on a Bruker WB 300. Then, the powdered sample was packed in a 4 mm diameter rotor and set to rotate at a speed up to 8 kHz with 63.669 resonance frequency in a Doty MAS probehead. During the whole acquisition time, the spinning rate of the rotor was locked to the required value using the Bruker pneumatic unit which controls both bearing and drive inlet nitrogen pressures. The ^{13}C spectrum was collected by a cross-polarization of proton with 5 ms contact time.

- **Hirshfeld surfaces**

Hirshfeld surface analysis is a powerful tool for obtaining additional information on the intermolecular interaction of molecular crystals. The size and the Hirshfeld surface form allow (allow) qualitative and quantitative investigation and visualization intermolecular close contacts in molecular crystals [44]. The 2D fingerprint of the Hirshfeld surface represents a new method for summarizing the complex information contained in a molecular crystalline structure in a single plot single color, which provides a "fingerprint" of intermolecular interactions in the crystal.

The combination of de and di in the form of a 2D fingerprint provides a summary of the contacts intermolecular in the crystal and complement the Hirshfeld surfaces [45]. Such parcels provide information on intermolecular transport interactions in the immediate environment of each molecule in the asymmetric unit.

3. Results and Discussions

3.1. Structural Resolution

XRD description:

The room temperature powder X-ray patterns of the (**I**) and (**II**) compounds are shown in **Figure 1**. The formation of pure phase for the both compounds without secondary phases has been confirmed. The peaks are fine, indicating that the samples are well crystallized. All the reflection peaks were indexed in the monoclinic system with the space group. All the reflection peaks were indexed in the monoclinic system with the space group C2/c. The lattice parameters were refined using the least-squares subroutine of a standard computer program. These refined lattice parameters of $C_6H_4(NH_3)_2{\cdot}Cl_2$ (**I**) and β-$[C_6H_{10}N_2]_2ZnCl_4$ (**II**) compounds are: a = 7.267 (7) Å; b = 14.403 (1) Å, c = 7.941 (1) Å, β = 94.568 (2)˚, V = 828.592 (2) Å^3; a = 7.411 (7) Å; b = 25.585 (1) Å, c = 9.342 (1) Å, β = 94.022 (2)˚ and V = 1776.93 (2) Å^3, respectively. The unit cell parameters are in good agreement with the single crystal X-ray values.

Structure description of $C_6H_4(NH_3)_2{\cdot}Cl_2$ compound (I):

The structure of $C_6H_4(NH_3)_2{\cdot}Cl_2$ compound (I) occurs as monoclinic crystals in the space group C2/c with each molecule occupying a general position within the unit cell. The unit asymmetric of compound (**I**) (**Figure 2**) consists of two isolated chloride atoms and half of the organic cation $[C_3H_5]^+$. A projection along the c-axis of the structure can be described by alternating $[C_6H_{10}N_2]^{2+}$ cationic layers and Cl^- anionic layers (**Figure 3**) through extensive intermolecular N-H···Cl interactions.

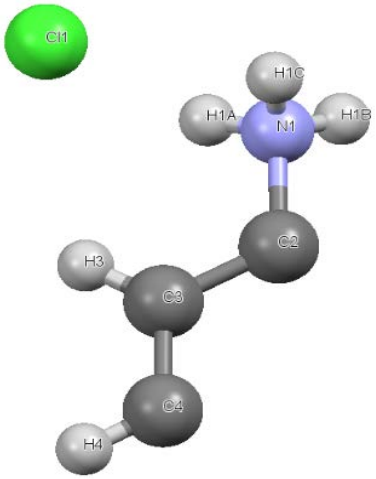

Figure 2. Unit asymmetric of $C_6H_4(NH_3)_2{\cdot}Cl_2$ (I) structure.

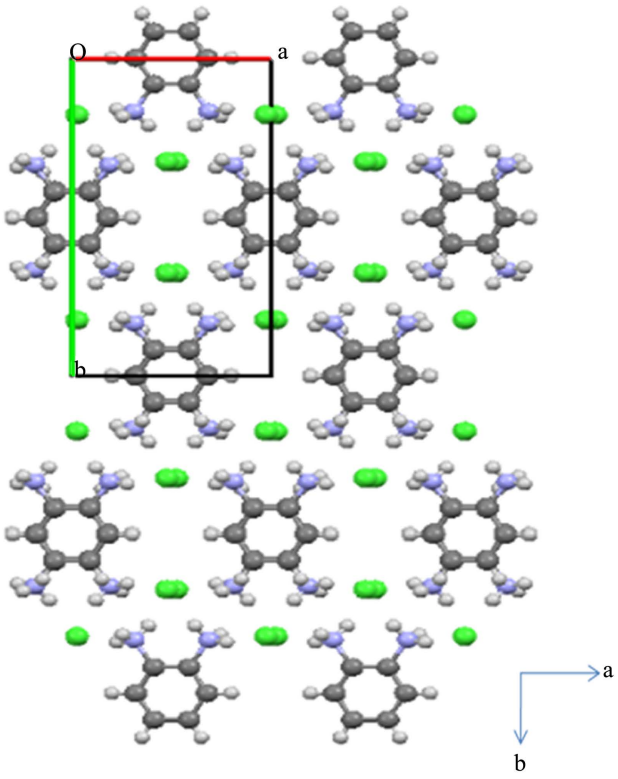

Figure 3. A projection, along the c axis, of the layers in the structure of $C_6H_4(NH_3)_2{\cdot}Cl_2$ (I).

Indeed, the pyridine rings of the original 1,2-benzen diammonium have undergone bi-protonation (H^+) during the synthesis process. The organic layer, observed at z/b = 1/4, is formed by the cations $[C_6H_{10}N_2]^{2+}$, arranged parallel plane in the direction a and interconnected via a p-p interaction.

In the half cation the C-C/C-N bonds are almost equivalent: C2-C3 = 1.3867 (2) Å; C3-C4 = 1.3929 (2) Å and C2-N1 = 1.4607 (2) Å. The C-C-C and C-C-N angles vary within the range from 119.40 (1)˚ and 119.815 (1), respectively. The main inter atomic distances and angles in the cation are reported in **Table 2**. These values are in agreement with those observed in similar compounds [46] [47] [48].

Indeed, the crystal packing is assured by three hydrogen bonds (N-H···Cl), N1-H1A···Cl1, N1-H1B···Cl1^{ii}, N1-H1C···Cl1^{iii} (for details and symmetry code, see **Table 3**).

Structure description of β-$[C_6H_{10}N_2]_2ZnCl_4$ compound (II):

The crystallographic analysis revealed that the complex (β-$[C_6H_{10}N_2]_2ZnCl_4$ (**I**)) crystallized in the monoclinic system, space group C2/c, involving the coordination of 1,2-benzen diammonium cation to the Zn^{2+} anions. It is a three-dimensional (3-D) structure with an asymmetric unit of one $[C_6H_{10}N_2]^{2+}$ cation and one $[ZnCl_4]^{2-}$ (**Figure 4**). Their following unit cell dimensions are grouped in **Table 1**.

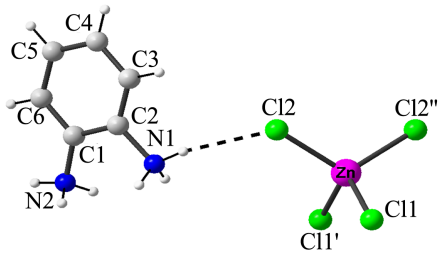

Figure 4. Unit asymmetric of β-$[C_6H_{10}N_2]_2ZnCl_4$ (II) structure.

Table 2. Principal interatomic distances (Å) and angles (˚) of organic groups of $C_6H_4(NH_2)_2{\cdot}2HCl$ (I).

	Distances (Å)		Angles (˚)	
Cation	N1-C2	1.460 (2)	C3-C2-N1	118.66 (1)
	C2-C3	1.386 (2)	C3-C2-N1	120.97 (1)
	C3-C4	1.392 (2)	C2-C3-C4	119.40 (2)

Table 3. Hydrogen bonds in the structure (I) (Å and ˚).

D-H	d(D-H)	d(H···A)	<DHA	d(D···A)
N1-H1A···Cl1	0.88 (3)	2.294	166.22	3.104 (6)
N1-H1B···Cl1^{ii}	0.88 (3)	2.266	168.24	3.104 (6)
N1-H1C···Cl1^{iii}	0.89 (3)	2.314	151.34	3.092 (5)

Codes de Symétrie: (ii) $-x+3/2, -y+1/2, -z+1$; (ii) $-x+1, y, -z+1/2$.

Projections along the c-axis of the structure present tetrahedral layers, $[ZnCl_4]^{2-}$, sandwiched between two layers of pyridinium cations $[C_6H_{10}N_2]^{2+}$ (**Figure 5(a)**).

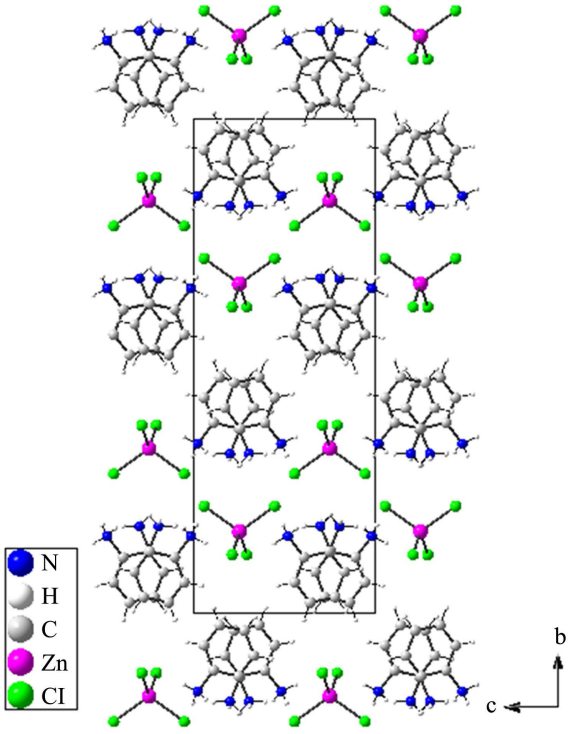

(a)

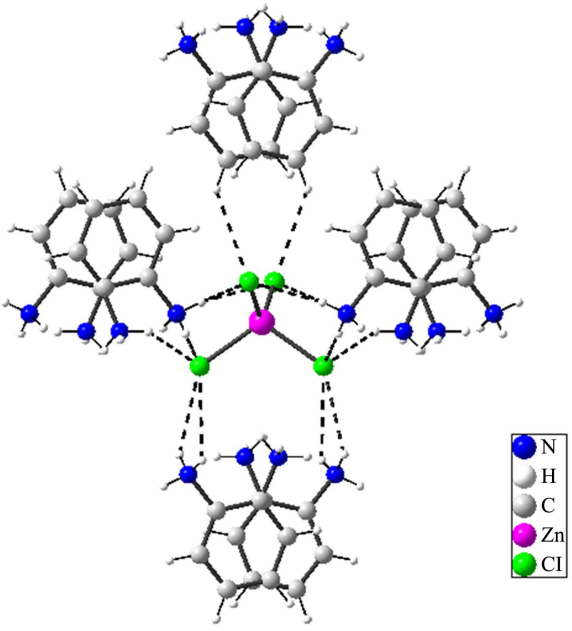

(b)

Figure 5. Packing diagram of β-$[C_6H_{10}N_2]_2ZnCl_4$ (II) viewed parallel to the a-axis (a). All atoms are shown as spheres of arbitrary size. Dashed lines represent N-H···Cl contacts from hydrogen bonds (b).

The organic part is formed by a single type of cation $[C_6H_{10}N_2]^+$ (**Figure 5(a)** and **Figure 5(b)**). The main details of interatomic distances and angles are summarized in **Table 4**. Bond distances and angles in the cations are normal [49] [50], with average of C-C = 1.389 (*6*)Å, C-N = 1.439 (*5*)Å, C-C-C = 119.998 (*3*)˚ and C-C-N = 120.035 (2)˚. The small angle is of the order of 117.67 (2) presents a small variant with that observed in benzene, this is due to the link N-H···Cl. Protonation double in N influences the angles, which indicates flattening of the benzene.A similar behaviour was noticed earlier for quinine and cinchonine [51] [52]. Furthermore, an influence of the proton (H^+), attached to the nitrogen atome (N1 or N2), on the surrounding of this atom may be estimated by a parameter called pyramidality [53]. The C-C distances equal to 1.383 Å and C-C-C angles equal to 120˚ [54]. This variation is due to the existence of intermolecular interactions. The protonation in the N site is well confirmed by the C-NH_3 bond length, in fact the distance C1-N2 is equal to 1.413 (2) Å, which is significantly longer than in the case of the C-NH2 molecule (CN = 1.335 (3)) [55], the CCN angles range from 119.01 (2)˚ to 121.45 (2)˚.

Geometry and coordination of the anion $[ZnCl_4]^{2-}$:

The inorganic layer is made up of $[ZnCl_4]^{2-}$ tetrahedral, observed at z/c = *1/4* and z/c = *3/4* (**Figure 5(a)**). The four distances between Zn-Cl ranged from *2.2561* (*4*) to *2.2938* (*4*)Å. They are equivalent two to two. Six Cl-Zn-Cl angles are varied between *105.155* (*16*)˚ and *115.72* (*3*)˚. They are grouped by three, two and a wide angle of the order of 115.72 (3) (for details see **Table 5**). These values are in agreement with those observed in similar compounds [56] [57] [58] [59].

From the geometric parameters, the $[ZnCl_4]^{2-}$ anion has a slightly distorted tetrahedral stereochemistry. The Baur distortion indices [60] can be calculated using the expressions:

Table 4. Principal interatomic distances (Å) and angles (˚) of organic groups of *β*-$[C_6H_{10}N_2]_2ZnCl_4$ (II).

	Distances (Å)		Angles (˚)	
Cation	N1-C2	1.466 (2)	C3-C2-N1	119.01 (2)
	N2-C1	1.413 (2)	C1-C2-N1	119.03 (2)
	C2-C3	1.390 (3)	C2-C1-N2	121.45 (2)
	C2-C1	1.393 (2)	C6-C1-N2	120.65 (2)
	C3-C4	1.382 (2)	C3-C2-C1	121.91 (2)
	C4-C5	1.391 (3	C4-C3-C2	119.65 (2)
	C5-C6	1.386 (3)	C3-C4-C5	119.27 (2)
	C6-C1	1.396 (3)	C6-C5-C4	120.82 (2)
			C5-C6-C1	120.67 (2)
			C2-C1-C6	117.67 (2)

$$ID(\text{Zn-Cl}) = \sum_{i=1}^{n_2} \frac{|d_i - d_m|}{n_1 d_m};\ ID(\text{Cl-Zn-Cl}) = \sum_{i=1}^{n_2} \frac{|a_i - a_m|}{n_2 a_m};$$

where d is the (Zn-Cl) distance, a is the (Cl-Zn-Cl) angle, m is the average value, $n_1 = 4$, and $n_2 = 6$. The values of these indices were *0.00206* and *0.00438*, respectively.

Hydrogen bonding interactions

The assembly between inorganic and organic entities in the isostructural compounds is provided by hydrogen bonds of the N-H···Cl type. Hence, these interactions have a crucial role in the formation of 3D supramolecular structures. The hydrogen bond parameters are given in Table 3 and Table 6.

For the compound (**I**), the N···Cl distances are between 3.093 Å and 3.105 Å and the H···Cl distances are in the range of 2.266 Å to 2.314 Å. However the NH···Cl angles vary between 151.34˚ and 168.24˚ (Table 3).

For the compound (**II**), the greatest N···Cl distance is 3.712 (2) Å and the H···Cl distances are in the range of 2.40 (3) Å to 2.93 Å. However the NH···Cl angles vary between 113.4 (2)˚ and 161 (2)˚. Whereas the N-H angle···N is in the range 123˚ and 153˚ (Table 6). It is deduced that the NH···N hydrogen bonds are moderate [61] [62] [63] [64] [65].

Table 5. Principal interatomic distances (Å) and angles (˚) of inorganic groups of $[ZnCl_4]^{2-}$.

	Distances (Å)		Angles (˚)	
Cation	Zn1-Cl2	2.256 (4)	Cl2-Zn1-Cl2	115.72 (3)
	Zn1-Cl2	2.256 (4)	Cl2-Zn1-Cl1	105.15 (2)
	Zn1-Cl1	2.293 (4)	Cl2-Zn1-Cl1	110.27 (2)
	Zn1-Cl1	2.293 (4)	Cl2-Zn1-Cl1	110.27 (2)
			Cl2-Zn1-Cl1	105.15 (2)
			Cl2-Zn1-Cl1	110.31 (2)

Table 6. Hydrogen bonds in the structure (II) (Å and ˚).

D-H···*A*	*D*—H	H···*A*	*D*···*A*	*D*—H···*A*
N1-H1*A*···N2^{ii}	0.84 (3)	2.20 (3)	2.970 (2)	153 (2)
N1-H1*A*···Cl1^{iii}	0.84 (3)	2.83 (2)	3.2563 (2)	113.4 (2)
N1-H1*B*···Cl1^{iv}	0.92 (3)	2.40 (3)	3.2854 (2)	161 (2)
N1-H1*C*···Cl2	0.89 (3)	2.44 (3)	3.2589 (17)	154 (2)
N1-H1*C*···Cl2^{iv}	0.89 (3)	2.88 (2)	3.3485 (18)	115.0 (2)
C6-H6···Cl2^{ii}	0.95	2.93	3.712 (2)	140.1
N2-H2*A*···Cl1^{v}	0.91	2.63	3.4089 (17)	143.8
N2-H2*B*···N1^{ii}	0.91	2.38	2.970 (2)	123
N2-H2*B*···N2^{ii}	0.91	2.62	3.427 (3)	147.8

The comparison between the angles NH···Cl, allowed us to note that those of the compound (II) are larger. These are due to the chlorine atoms bound to the Zinc atom, against the chlorine of the first compound is free.

Based on values of **Table 3** and **Table 5**, it can be concluded that the hydrogen bonds are weak [66]. The cations are connected to each other by π-π stacking interactions are of fundamental importance for the further development of supramolecular components and prediction of their crystal structures.

3.2. Surface De Hirchfeld

Hirchfeld surfaces, which define the electron density weighing the boundary surfaces between molecules in a crystal, are useful for analyzing and displaying intermolecular contacts [67].

The Hirshfeld surfaces of the both compounds are showed in **Figure 6** and **Figure 7**. Hirchfeld molecular surface calculations were performed using the Crystal program Explorer [68] [69], CIF files have been registered in this program. Hirchfeld surfaces are calculated using the following equation:

$$d_{norm} = \frac{d_i - r_i^{vdw}}{r_i^{vdw}} + \frac{d_e - r_e^{vdw}}{r_e^{vdw}}$$

where, d_e is the distance between the Hirshfeld surface and the nearest atom outside the surface, d_i is the distance between the Hirshfeld surface and the nearest atom inside the surface, d_{norm} is expressed as a function of d_e and d_i and the radius of Van Der Waals atoms. The d_{norm} value is negative or positive when the intermolecular contacts are shorter or longer than the Van Der Waals (VDW) rays, respectively. The Hirshfeld surface uses a red-blue-white color scheme: the red regions represent the closest contacts and a negative reference value; the blue regions represent longer contacts and a positive d_{norm} value; and the white regions represent a contact distance exactly equal to the VDW separation with a d_{norm} value of zero [70].

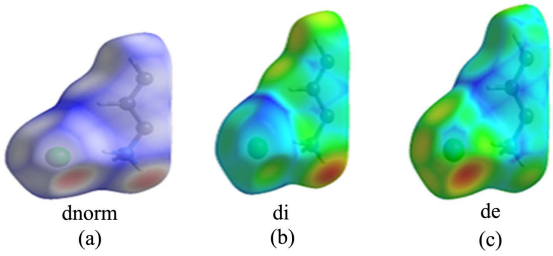

Figure 6. Hirshfeld surface analysis of $C_6H_4(NH_2)_2{\cdot}HCl$, d_{norm} (a) di (b) de (c).

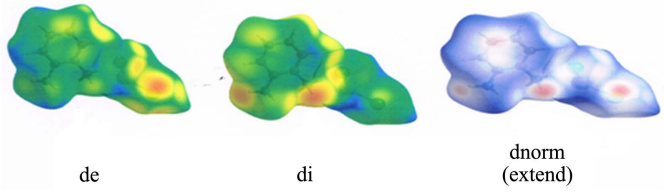

Figure 7. Hirshfeld surface analysis of β-$[C_6H_{10}N_2]_2ZnCl_4$ (II), d_{norm}, di and de.

D fingerprints of the Hirshfeld surface of the study structure to highlight atoms involved in close contact [71] [72].

Figure 8 illustrates the 2D fingerprint of all the contacts contributing to the Hirshfeld surface of $C_6H_4(NH_2)_2{\cdot}HCl$ (**I**) compound. The graph in **Figure 9** illustrates the 2D Fingerprint of all the contacts contributing to the Hirshfeld surface of β-$[C_6H_{10}N_2]_2ZnCl_4$ (**II**) compound, associated with the hydrogen atoms.

These graphs represents the H-Cl/Cl-H contacts between the hydrogen atoms located inside the Hirshfeld surface and the externally located in chlorine atoms and vice versa. The H-Cl/Cl-H contacts have the largest contribution to the total Hirshfeld surface (41.9%).

In the crystallization of these compounds, intermolecular interactions of the H···ClCl···H and H···H type are the most abundant. It is evident that van der Waals forces exert an important influence on the stabilization of packing in the crystal structure. While other interconnects contribute less to Hirshfeld surfaces: H-C/C-H (7.6%) (**Figure 8(c)**). However, the contacts Cl-Cl (**Figure 8(f)**), C-Cl/C-Cl (**Figure 8(f)**) and N-H/H-N (**Figure 8(g)**) have contributions of very small percentages of interactions (*0.6*%), (*0.1*%) and (*0.2*%), respectively.

In order to give some insight into the nature of forces stabilizing the discussed structures, the intermolecular interactions were analyzed with the help of Hirshfeld surface. **Figure 9** present the 3D Hirshfeld surface and 2D fingerprint histogram of the title molecule of for the β-$[C_6H_{10}N_2]_2ZnCl_4$ (**II**). This state indicates presence of the C-H···Cl type intermolecular hydrogen bond interactions in crystal structure. The C-H···Zn type intermolecular hydrogen bond distances in crystal. Similarly, as seen from crystallographic analysis, the contact distances between Cl are obtained between and hydrogen atoms have considerable small values and the Cl-H/H-Cl interactions contribute to Hirshfeld surface with 34.2% value. The major contributions to Hirshfeld surface are H-H with *32.2*% and C-H/H-C with 7.3%. The fingerprint of β-$[C_6H_{10}N_2]_2ZnCl_4$ (**II**) compound, suggest that the H···H and C···H contacts dominate the crystal interactions. However, these interactions present higher interatomic distance. Interactions with less interatomic distance (stronger interactions) are observed in fingerprint plots as pointy regions. The H···H contacts are present in higher percentages on the surface probably due to the close packing, resulting in the greater proximity between the molecules in the crystal arrangements. The contacts C···H present contributions with close values in the crystalline forms, smaller in polymorph II. The wings represent contacts C-H···π, present in all cases.

3.3. Spectroscopy Studies

Figure 10 and **Figure 11** present the infrared spectra of $C_6H_4(NH_3)_2{\cdot}Cl_2$ (I) and β-$[C_6H_{10}N_2]_2ZnCl_4$ (II) at ambient temperature; respectively; to give more information on the crystal structure. A band at 3400 cm^{-1}, attributed to asymmetric, stretching vibration νas (NH_3), and a less intense band at 3370 cm^{-1} relative to the symmetrical elongation vibration νs (NH_3). The modes of vibration (C-H) of the benzene nucleus appear at 3220 cm^{-1} and 2800 cm^{-1}.

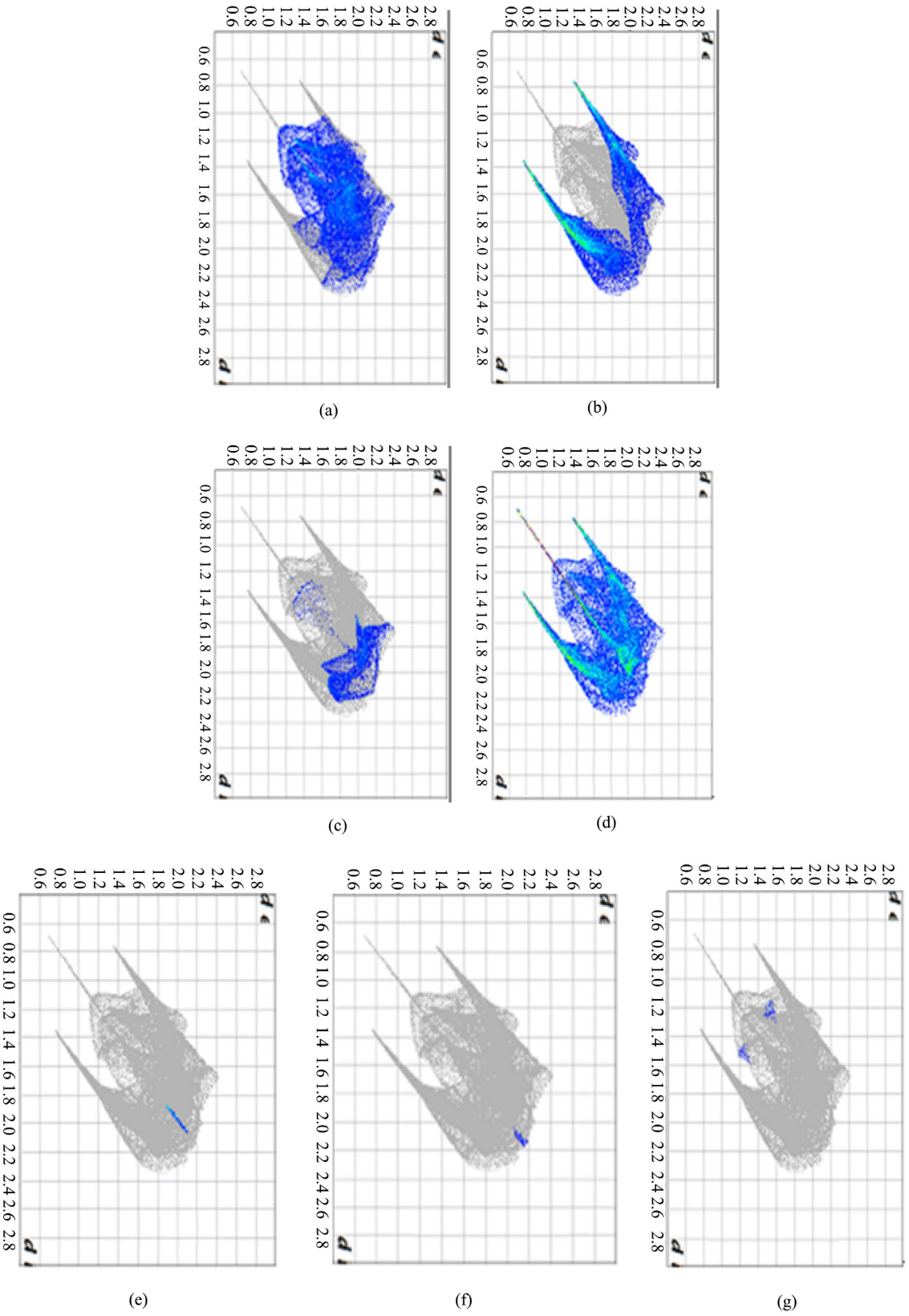

Figure 8. Fingerprint of all the contacts contributing to the Hirshfeld surface of $C_6H_4(NH_2)_2$·HCl (I) compound: (a) H-H contacts, (b) HCl/HCl, (c) H-C/C-H, (d) all intermolecular contacts, (e) Cl-Cl, (f) C-Cl/Cl-C and (g) N-H/H-N.

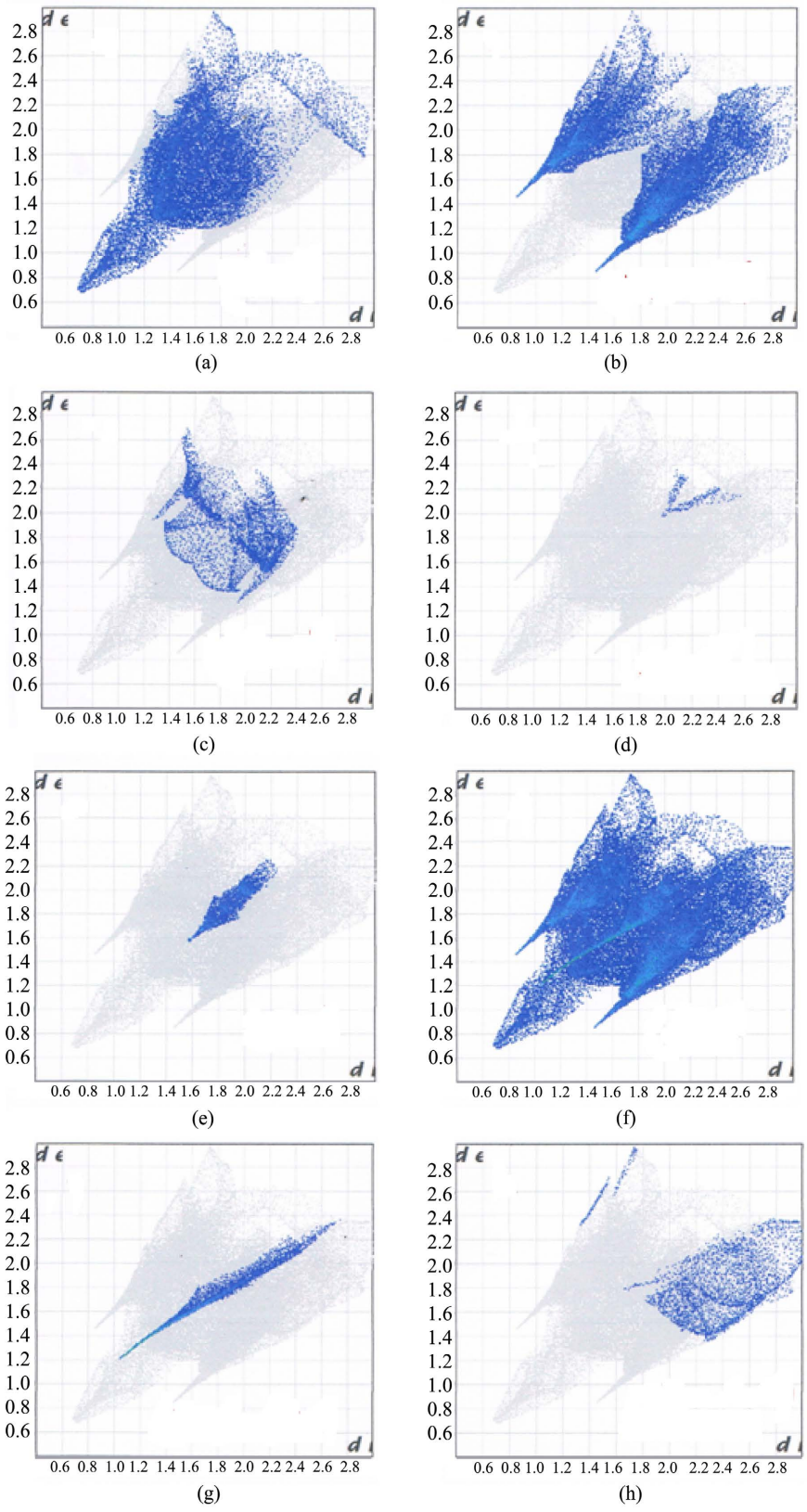

Figure 9. Fingerprint of all the contacts contributing to the Hirshfeld surface of β-$[C_6H_{10}N_2]_2ZnCl_4$ (II) compound. (a) HC-CH, (b) HCl/ClH, (c) HC/CH, (d) CCl/ClC, (e) C-C, (f) All, (g) ZnCl-ClZn, (h) HZn-ZnH.

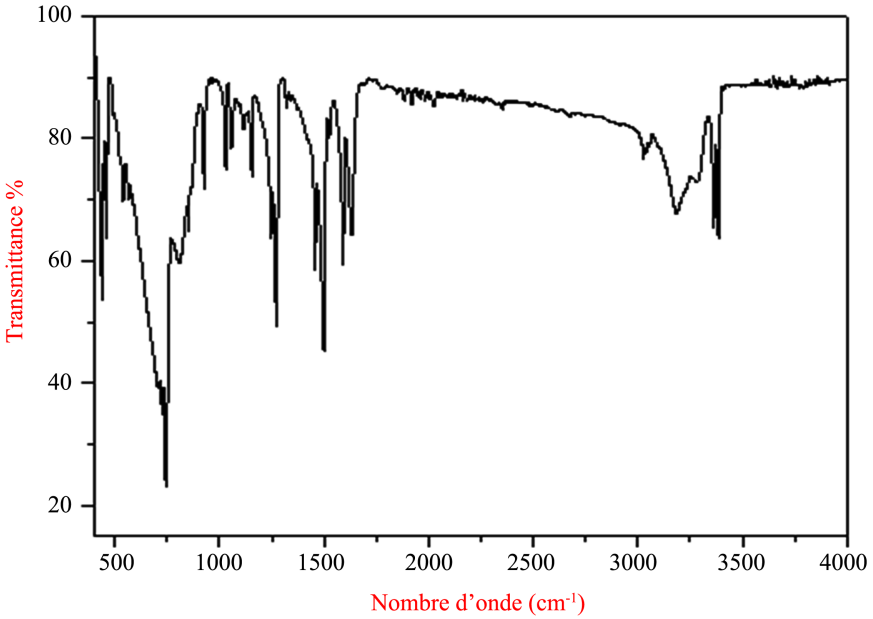

Figure 10. FT-IR spectra of $C_6H_4(NH_3)_2{\cdot}Cl_2$ (I) at room temperature.

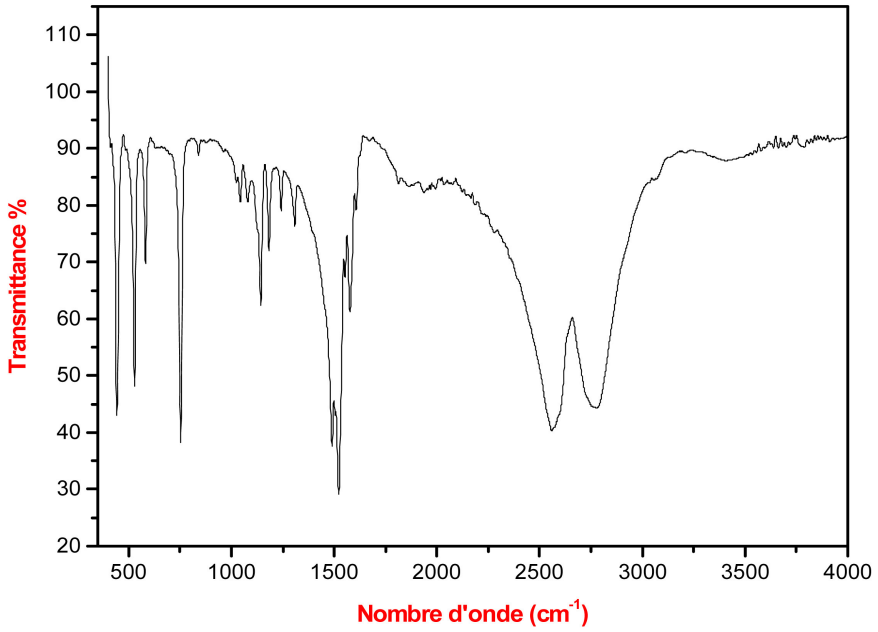

Figure 11. FT-IR spectra of β-$[C_6H_{10}N_2]_2ZnCl_4$ (II) at room temperature.

The band at 1497 cm^{-1} is attributed to C = C elongation vibration and the two vibration bands (C-C) are located between 1500 cm^{-1} and 1526 cm^{-1}. Two bands: one at 1253 cm^{-1} relative to asymmetric valence vibration νas (C-N) and the other less intense at 1189 cm^{-1} correspond to symmetric valence vibration νs (C-N). The more intense band at 778 cm^{-1} attributed the off-plane aromatic (CH) bond, while the two moderately intense bands in the 479 - 515 cm^{-1} frequency range corresponds respectively to δ (CCN) and torsion outside the plan of the group NH_3. We conclude that infrared spectroscopy confirms the pres-

ence of the $[C_6H_4(NH_2)]^{2+}$ cationic part of our compound $C_6H_4(NH_3)_2{\cdot}Cl_2$ (**I**) [73] [74] [75] [76] [77].

The IR spectrum has several bands that can be assigned as follows:

- The bands observed at high frequency between 3550 and 3800 cm^{-1} in IR is related to symmetrical and asymmetric stretching of an amine group (NH_2). In addition, the observed groups in 3100, 3300 cm^{-1} in IR are attributed to symmetric and asymmetric NH stretching.

A wide band containing two signals, one around 2800 cm^{-1} and the other at 2550 cm^{-1}, correspond to the elongation vibrations of (=C-H).

- The bung, which is located at 1620 cm^{-1} is probably due to the shear vibration of δ (NH_2) which is combined with (N-H) + of the symmetrical plane (sway) appearing at 1500 cm^{-1}.
- The elongation vibration (C = C) is observed at 1498 cm^{-1}. Stretching vibrations (C-C) were observed at 1250 cm^{-1}. A stretching, vibration (C-N) appeared at 1200 cm^{-1}. The symmetrical off-plane vibration (C-H) (C-H wagging oop) created a band at 750 cm^{-1}.
- The band observed at 738 cm^{-1} is attributed to (C-C) torsional vibration. Finally, the intense peak that appeared at 450 cm^{-1} is due to the band (C-N) in the plane of flexion.
- The bands observed at 450 cm^{-1} correspond to (C-C-C) in the plane.

In conclusion, the infrared study only confirms the presence of the organic group $[C_6H_9N_2]^{2+}$.

3.4. NMR Study

The experimental spectrum (in blue) and the spectrum obtained by smoothing, using the β-DMFIT software (in red) are shown in **Figure 12**.

The isotropic band of ^{13}C CP-MAS-NMR spectrum of the crystalline powder sample rotating at the magic angle with frequency 8 kHz illustrated in **Figure 11**. Spinning the sample at different frequencies allows us to identify the isotropic band. The spectrum is composed of three isotropic bands P1, P2 and P3. Simulation of the isotropic bands permits to identify twelve peaks using Gaussian-Lorentzian functions by means of a Dmfit program [43] (**Table 7**). The deconvolution of three signal shows confirm that the nitrogen-bonded atoms (heteroatom) with a higher electronegativity undergo the phenomenon of shielding consequently these carbon atoms move towards the high chemical shifts in ppm, correspond to the P1 band (to 268.83 at 135.74 ppm). The least shielded peaks observed towards the low ppm; P2 band (130.97 at 117.28 ppm) correspond to the ring carbon atoms not bound to the most unshielded carbon nitrogen atoms; P3 band (108.82 - 87.75 ppm) (**Table 7**). The chemical shift values were commonly observed in similar compounds [78] [79].

This study shows that the compound consists of organic groups that have non-equivalent carbons. This result will be confirmed by the study of single-crystal X-rays.

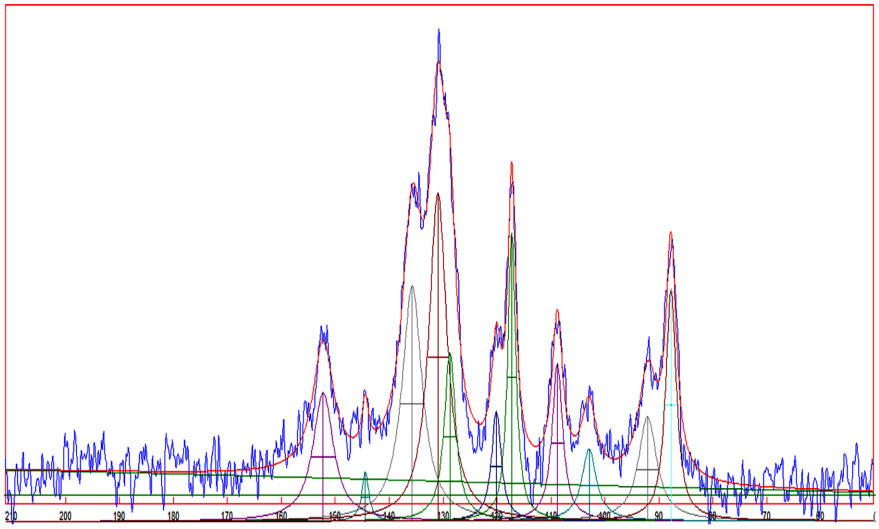

Figure 12. Deconvolution of isotropic band of ^{13}C spectrum of β-$[C_6H_{10}N_2]_2ZnCl_4$ (II).

Table 7. ^{13}C cross-polarization NMR MAS of the synthesized compound at 8 kHz.

Position (ppm)		Width Δ (ppm)
268.83	P1	4.56
152.24		4.65
144.43		1.55
135.74		4.53
130.97	P2	4.00
128.73		2.55
120.14		2.15
117.28		1.77
108.82	P3	2.39
102.94		3.30
92.09		4.16
87.75		2.37

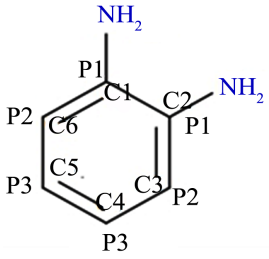

4. Conclusion

In conclusion, the study of newly-prepared hybrids $C_6H_4(NH_3)_2{\cdot}Cl_2$(**I**) and β-$[C_6H_{10}N_2]_2ZnCl_4$ (**II**) compounds. This study has revealed that new both compounds were found to crystallize in the same crystalline system and the same space group; monoclinic C2/c. Whose their structural arrangements can be described as an alternation of organic-inorganic layers, are performed via N-H···Cl hydrogen bonding and π-π stacking interactions. Hirshfeld surface analysis reveals the percentage of intermolecular contacts of the both compounds. Furthermore, the infrared study confirms the presence of the organic group $[C_6H_9N_2]^{2+}$. Moreover, Solid state NMR spectra showed three isotropic bands P1, P2 and P3,

correspond to the non-equivalent carbon atoms. Thus confirming the solid state structure determined by X-ray diffraction.

Acknowledgements

This work was supported by the Ministry of Higher Education and Scientific Research in Tunisia, Univ Rennes, CNRS, ISCR (Institute des Sciences Chimiques de Rennes) and National Center for Research in Materials Science (CNRSM), laboratory for the valorization of useful materials (LVMU), Borj cedria in Tunisia.

Conflicts of Interest

The authors declare no conflicts of interest regarding the publication of this paper.

References

[1] Vishwakarma, A.K., Kumari, R., Ghalsasi, P.S. and Arulsamy, N. (2017) Crystal Structure, Thermochromic and Magnetic Properties of Organic-Inorganic Hybrid Compound: $(C_7H_7N_2S)_2CuCl_4$. *Journal of Molecular Structure*, **1141**, 93-98. https://doi.org/10.1016/j.molstruc.2017.03.076

[2] Vincent, V.Ch., Kirubavathi, K., Bakiyaraj, G. and Selvaraju, K. (2019) Experimental and Theoretical Investigations of 4-Hydroxy L-Proline Cadmium Chloride Nonlinear Optical Crystal. *Spectrochimica Acta*, *Part A*: *Molecular and Biomolecular Spectroscopy*, **212**, 61-70. https://doi.org/10.1016/j.saa.2018.12.037

[3] Rok, M., Piecha-Bisiorek, A., Szklarz, P., Bator, G. and Sobczyk, L. (2015) Electric Response in the Antiferroelectric Crystal of 4,4'-di-t-butyl-2,2'-bipyridyl with Chloranilic Acid. *Chemical Physics*, **452**, 53-60. https://doi.org/10.1016/j.chemphys.2015.02.018

[4] Zhang, S. and Lanty, G. (2009) Synthesis and Optical Properties of Novel Organic-Inorganic Hybrid Nanolayer Structure Semiconductors. *Acta Materialia*, **57**, 3301-3309. https://doi.org/10.1016/j.actamat.2009.03.037

[5] Mkaouar, I., Karaa, N., Hamdi, B. and Zouari, R. (2016) Synthesis, Crystal Structure, Thermal Analysis, Vibrational Study Dielectric Behaviour and Hirshfeld Surface Analysis of $[C_6H_{10}(NH_3)_2)]_2SnCl_6(Cl)_2$. *Journal of Molecular Structure*, **1115**, 16. https://doi.org/10.1016/j.molstruc.2016.02.070

[6] Kchaou, H., Karoui, K., Bulou, A., *et al.* (2017) Raman Scattering and Alternative Current Conduction Mechanism of the Different Phase Transitions in $[(CH_3)_3NH]CoCl_3{\cdot}2H_2O$. *Journal of Alloys and Compounds*, **723**, 301-310. https://doi.org/10.1016/j.jallcom.2017.06.237

[7] Lassoued, M.S., Abdelbaky, M.S.M., Lassoued, A., *et al.* (2018) Structure Characterization, Photoluminescence and Dielectric Properties of a New Hybrid Compound Containing Chlorate Anions of Zincate(II). *Journal of Molecular Structure*, **1155**, 536-547. https://doi.org/10.1016/j.molstruc.2017.11.023

[8] Tian, C., Zhang, H. and Du, S. (2014) Acentric and Chiral Heterometallic Inorganic-Organic Hybrid Frameworks Mediated by Alkali or Alkaline Earth Ions: Synthesis and NLO Properties. *CrystEngComm*, **16**, 4059-4068. https://doi.org/10.1039/c3ce42419g

[9] Hfidhi, N., Kammoun, O., Bataille, T. and Naili, H. (2021) Structure Evolution and

Thermal Decomposition of Supramolecular and Lamellar Hybrid Sulfates Templated by 4-Aminopyridinium. *Journal of Inorganic and Organometallic Polymers and Materials*, **31**, 4165-4176. https://doi.org/10.1007/s10904-021-02089-9

[10] Slabbert, C. and Redemeyer, M. (2016) Structures and Trends of Neutral MX_xsolvent$_{4-x}$tetrahedra and Anionic $[MX_4]^{2-}$ Tetrahalometallates of Zinc(II), Cadmium(II) and Mercury(II) with Benzopyridine- and Benzopyrazine-Type N-Donor Ligands or Cations. *CrystEngComm*, **18**, 4555-4579. https://doi.org/10.1039/C6CE00568C

[11] Elwej, R. and Hlel, F. (2016) Hydrothermal Synthesis, Characterization by Single Crystal XRD, Structural Discussion and Electric, Dielectrical Properties of $(C_6H_9N_2)_2(Hg_{0.12}Zn_{0.88})Cl_4$ Hybrid Compound. *Physica E*: *Low-Dimensional Systems and Nanostructures*, **84**, 498-504. https://doi.org/10.1016/j.physe.2016.07.009

[12] Wang, X., Qin, Ch., Wang, E., *et al.* (2004) Syntheses, Structures, and Photoluminescence of a Novel Class of d10 Metal Complexes Constructed from Pyridine-3,4-dicarboxylic Acid with Different Coordination Architectures. *Inorganic Chemistry*, **43**, 1850-1856. https://doi.org/10.1021/ic035151s

[13] Bouaziz, E., Ben Hassen, C., Chniba-Boudjada, N., *et al.* (2017) Crystal Structure, Hirshfeld Surface Analysis, Vibrational, Thermal Behavior and UV Spectroscopy of (2,6-Diaminopyridinium) Dihydrogen Arsenate. *Journal of Molecular Structure*, **1145**, 121-131. https://doi.org/10.1016/j.molstruc.2017.05.043

[14] Elwej, R., Bulou, A. and Hlel, F. (2016) $(C_6H_9N_2)_2HgCl_4$(I), $(C_6H_9N_2)_2(Hg_{0.75}Cd_{0.25})Cl_4$(II) and $(C_6H_9N_2)_2(Hg_{0.12}Zn_{0.88})Cl_4$(III) Compounds: Syntheses, Crystal Structure and Spectroscopic Properties. *Synthetic Metals*, **222**, 372-382. https://doi.org/10.1016/j.synthmet.2016.11.008

[15] Chihaoui, N., Hamdi, B. and Zouari, R. (2017) Structural Elucidation, Theoretical Investigation Using DFT Calculations, Thermal and Dielectric Analyses of New Zinc(II) Based Inorganic-Organic Hybrid. *Chinese Chemical Letters*, **28**, 642-650. https://doi.org/10.1016/j.cclet.2016.10.002

[16] Mesbeh, R., Hamdi, B. and Zouari, R. (2017) Elaboration, Structural, Spectroscopy, DSC Investigations and Hirshfeld Surface Analysis of a One-Dimensional Self-Assembled Organic-Inorganic Hybrid Compound. *Journal of Molecular Structure*, **1128**, 205-2014. https://doi.org/10.1016/j.molstruc.2016.08.068

[17] Kundu, P., Chakraborty, P., Adhikary, J., *et al.* (2015) Influence of Co-Ligands in Synthesis, Photoluminescence Behavior and Catalytic Activities of Zinc Complexes of 2-((E)-((pyridin-2-yl)methylimino)methyl)phenol. *Polyhedron*, **85**, 320-328. https://doi.org/10.1016/j.poly.2014.08.011

[18] Xiao, L., Liu, Y., Xiu, Q., *et al.* (2010) Novel Polymeric Metal Complexes as Dye Sensitizers for Dye-Sensitized Solar Cells Based on Poly Thiophene Containing Complexes of 8-hydroxyquinoline with Zn(II),Cu(II) and Eu(III) in the Side Chain. *Tetrahedron*, **66**, 2835-2842. https://doi.org/10.1016/j.tet.2010.02.039

[19] Chan-on, W., Hyen, N.T.B., Songtaures, N., *et al.* (2015) Quinoline-Based Clioquinol and Nitroxoline Exhibit Anticancer Activity Inducing FoxM1 Inhibition in Cholangiocarcinoma Cells. *Drug Design, Development and Therapy*, **9**, 2033-2047. https://doi.org/10.2147/DDDT.S79313

[20] Cherdtrakulkiat, R., Boonpangrack, S., Sinthpoom, N., *et al.* (2016) Derivatives (Halogen, Nitro and Amino) of 8-Hydroxyquinoline with Highly Potent Antimicrobial and Antioxidant Activities. *Biochemistry and Biophysics Reports*, **6**, 135-141. https://doi.org/10.1016/j.bbrep.2016.03.014

[21] Khakhlary, P. and Baruah, J.B. (2015) Studies on Cluster, Salt and Molecular Complex of Zinc-Quinolinate. *Journal of Chemical Sciences*, **127**, 215-223.

https://doi.org/10.1007/s12039-015-0781-6

[22] Bush, A.I. (2004) Drug Resistance Updates. *Chemistry & Biology*, **4**, 347-364.

[23] Zhong, C., Wu, Q., Gwo, R. and Zhang, H. (2008) Synthesis and Luminescence Properties of Polymeric Complexes of Cu(II), Zn(II) and Al(III) with Functionalized Polybenzimidazole Containing 8-Hydroxyquinoline Side Group. *Optical Materials*, **30**, 870-875. https://doi.org/10.1016/j.optmat.2007.03.008

[24] Yuan, G., Shan, W., Chen, J., *et al.* (2005) Synthesis, Structure and Photophysical Properties of a Binuclear Zn(II) Complex Based on 8-Hydroxyquinoline Ligand with Naphthyl Unit. *Journal of Luminescence*, **160**, 16-21. https://doi.org/10.1016/j.jlumin.2014.11.017

[25] Chihaoui, N., Hamdi, B. and Zouari, R. (2017) Structural Elucidation, Theoretical Investigation Using DFT Calculations, Thermal and Dielectric Analyses of New Zinc(II) Based Inorganic-Organic Hybrid. *Chinese Chemical Letters*, **28**, 642-650. https://doi.org/10.1016/j.cclet.2016.10.002

[26] Karaa, N., Hamdi, B., Ben Salah, A. and Zouari, R. (2013) Synthesis, Infra-Red, CP/MAS-NMR Characterization, Structural Study and Electrical Properties of the Bis(4-amino-2-chloropyridinium) Tetrachlorozincate(II) Monohydrate. *Journal of Molecular Structure*, **1049**, 48-58. https://doi.org/10.1016/j.molstruc.2013.06.003

[27] Yamamoto, Y., Yoshida, T., Suzuki, T. and Kaizaki, S. (2011) *Inorganica Chimica Acta*, **325**, 187-194.

[28] Adams, H., Bradshaw, D. and Fenton, D.E. (2002) A Co-Ordination Number Asymmetric Dinuclear Zinc(II) Complex of an Unsymmetrical Compartmental Proligand. *Polyhedron*, **21**, 1957-1960. https://doi.org/10.1016/S0277-5387(02)01099-9

[29] Maldonado, C.R., Quiros, M. and Salas, J.M. (2008) Chlorocadmate(II) Salts of Two 1,2,4-triazolo-[1,5-a] Pyrimidine Derivatives. *Journal of Molecular Structure*, **882**, 30-34. https://doi.org/10.1016/j.molstruc.2007.09.004

[30] Jian, F.F., Zhao, P.S., Wang, Q.X. and Li, Y. (2006) One-Dimensional Cd Metal String Complex: Synthesis, Structural and Thermal Properties of $[(HPy)_3(Cd_3Cl_9)]_\infty$. *Inorganica Chimica Acta*, **59**, 1473-1477. https://doi.org/10.1016/j.ica.2005.10.054

[31] Thorn, A., Willett, R.D. and Twamley, B. (2006) Novel Series of Ribbon Structures in Dialkylammonium Chlorocadmates Obtained by Dimensional Reduction of the Hexagonal $CdCl_2$ Lattice. *Crystal Growth & Design*, **5**, 1134-1142. https://doi.org/10.1021/cg050584m

[32] Chaabane, I., Hlel, F. and Guidara, K. (2008) Synthesis, Infra-Red, Raman, NMR and Structural Characterization by X-Ray Diffraction of $[C_{12}H_{17}N_2]_2CdCl_4$ and $[C_6H_{10}N_2]_2Cd_3Cl_{10}$ Compounds. *PMC Physics B*, **1**, 11. https://doi.org/10.1186/1754-0429-1-11

[33] Schröder, L., Watkin, D.J., Cousson, A., *et al.* (2004) *CRYSTALS* Enhancements: Refinement of Atoms Continuously Disordered along a Line, on a Ring or on the Surface of a Sphere. *Journal of Applied Crystallography*, **37**, 545-550. https://doi.org/10.1107/S0021889804009847

[34] Czarnecki, P., Nawrocik, W., Pajaxk, Z. and Nawrocik, J. (1994) Ferroelectric Properties of Pyridinium Perchlorate. *Journal of Physics*: *Condensed Matter*, **6**, 4955-4960. https://doi.org/10.1088/0953-8984/6/26/017

[35] Bayar, I., Khedhiri, L., Soudani, S., *et al.* (2018) Crystal Structure, Quantum Mechanical Investigation, IR and NMR Spectroscopy of Two New Organic Salts: $(C_8H_{12}NO)\cdot[NO_3]$(I) and $(C_8H_{14}N_4)\cdot[ClO_4]_2$(II). *Journal of Molecular Structure*, **1161**, 185-193. https://doi.org/10.1016/j.molstruc.2018.02.032

[36] (2014) APEX2 Program Suite, 11-0. Bruker AXS Inc., Madison.

[37] Sheldrick, G.M. (2013) SAINT, Version 8.37A. Bruker AXS Inc., Madison.

[38] Sheldrick, G.M. (2014) SADABS Version. Bruker AXS Inc., Madison.

[39] Farrugia, L.J. (1999) W*inGX* Suite for Small-Molecule Single-Crystal Crystallography. *Journal of Applied Crystallography*, **32**, 837-838. https://doi.org/10.1107/S0021889899006020

[40] Altomare, A., Burla, M.C., Camalli, M., *et al.* (1999) SIR97: A New Tool for Crystal Structure Determination and Refinement. *Journal of Applied Crystallography*, **32**, 115-119. https://doi.org/10.1107/S0021889898007717

[41] Sheldrick, G.M. (2014) SHELXL-2014/1, Program for Crystal Structure Refinement. University of Göttingen, Göttingen, 71, 3-8.

[42] Brandenburg, K. (2006) DIAMOND. Crystal Impact GbR, Bonn.

[43] Massiot, D. and Theile, H. (1994) Germany, Bruker Rep 140, 43-46.

[44] McKinnon, J.J., Jayatilaka, D. and Spackman, M.A. (2007) Towards Quantitative Analysis of Intermolecular Interactions with Hirshfeld Surfaces. *Chemical Communications*, **37**, 3814-3816. https://doi.org/10.1039/b704980c

[45] Spackman, M.A. and Jayatilaka, D. (2009) Hirshfeld Surface Analysis. *CrystEngComm*, **11**, 19-32. https://doi.org/10.1039/B818330A

[46] Haddad, S.F., Ali, B.F. and Al-Far, R. (2012) 2-Amino-5-methyl-pyridinium Dibromoiodate. *Acta Crystallographica Section E*, **68**, 2786. https://doi.org/10.1107/S1600536812036136

[47] Sehimi. H., Akitsuc, T. and Zid, M.F. (2019) Synthesis and Structural Study of Tris-(2,6-diaminopyridinium) bis(oxalato)dioxidovanadate(V)2.5-hydrate. *Acta Crystallographica Section E*, **75**, 680-684. https://doi.org/10.1107/S2056989019005267

[48] Bringley, J.F. and Rajeswaran, M. (2006) p-Phenylenediammonium Tetrachlorozincate(II). *Acta Crystallographica Section E*, **62**, m1304-m1305. https://doi.org/10.1107/S1600536806016837

[49] Elwej, R., Bulou, A. and Hlel, F. (2016) $(C_6H_9N_2)_2HgCl_4$(I), $(C_6H_9N_2)_2(Hg_{0.75}Cd_{0.25})Cl_4$(II) and $(C_6H_9N_2)_2(Hg_{0.12}Zn_{0.88})Cl_4$(III) Compounds: Syntheses, Crystal Structure and Spectroscopic Properties. *Synthetic Metals*, **222**, 372-382. https://doi.org/10.1016/j.synthmet.2016.11.008

[50] Feddaoui, I., Abdelbaky, M.S.M., Granda, S.G., *et al.* (2019) Synthesis, Crystal Structure, Physico-Chemical Characterization and Theoretical Study of a New Pb(II) Complex $[C_{10}H_{22}N_2]_3{\cdot}PbCl_5{\cdot}3Cl{\cdot}3H_2O$. *Journal of Molecular Structure*, **1185**, 259-267. https://doi.org/10.1016/j.molstruc.2019.02.111

[51] Kowalik, J.T., Lipinska, T., Oleksyn, B.J. and Sliwinski, J. (1999) Conformation of Epicinchonine and Cinchonine in View of Their Antimalarial Activity: X-Ray and Theoretical Studies. *Enantiomer*, **4**, 389-410.

[52] Wesełuch, A., Ska, B., Oleksyn, B.J., *et al.* (2005) Crystal Structure and EPR Studies of $(cinchonineH_2)_2(CdCl_4)$(Cd/$CuCl_4$) Crystals with Thermochromic and Jahn-Teller Effect. *Journal of Molecular Structure*, **751**, 109-120. https://doi.org/10.1016/j.molstruc.2005.05.004

[53] Hafelinger, G. and Mach, H.G. (1994) Enamines: General and Theoretical Aspects. In: Rappapor, Z., Ed., *The Chemistry of Enamines*, Wiley, New York, 13. https://doi.org/10.1002/0470024763.ch1

[54] Hlel, F., Thouvenot, R. and Smiri, L. (2005) Synthesis and Structural Characterization by ^{31}P MAS NMR and X-Ray Diffraction of the 3-Phenylpropylamonium Cyclohexaphosphate Dihydrate. *Physica Status Solidi* (*b*), **242**, 1243-1253. https://doi.org/10.1002/pssb.200406928

[55] Goswami, S., Mahapatra, A.K., Ghosh, K., *et al.* (1999) 2-Acetylamino-6-methylpyridine N-oxide Monohydrate. *Acta Crystallographica Section C*, **55**, 579-581. https://doi.org/10.1107/S0108270198014139

[56] Lassoued, M.S., Abdelbaky, M.S.M., Ben Soltan, W., *et al.* (2018) Structure Characterization, Photoluminescence and Dielectric Properties of a New Hybrid Compound Containing Chlorate Anions of Zincate(II). *Journal of Molecular Structure*, **1158**, 221-228. https://doi.org/10.1016/j.molstruc.2018.01.027

[57] Ben Gzaiel, M., Oueslati, A., Chaabane, I. and Gargouri, M. (2016) Density Functional Theory Calculations of the Molecular Structure and the Vibrational Spectra of Bis-Tetrapropyl-Ammonium Hexachloro-Dizincate. *Journal of Molecular Structure*, **1122**, 280-289. https://doi.org/10.1016/j.molstruc.2016.05.097

[58] Souissi, S., Smirani, W. and Rzaigui, M. (2009) Bis(2,5-Dimethylanilinium) Tetrachloridozincate(II). *Acta Crystallographica Section E Structure Reports Online*, **65**, m442. https://doi.org/10.1107/S1600536809009982

[59] Rayes, A., Mezzadri, F., Issaoui, N., *et al.* (2019) Synthesis, Physico-Chemical Studies, Non-Linear Optical Properties and DFT Calculations of a New Non-Centrosymmetric Compound: (3-ammoniumpyridinium)tetrachloridozincate (II). *Journal of Molecular Structure*, **1184**, 524-531. https://doi.org/10.1016/j.molstruc.2018.12.042

[60] Baur, W. (1974) The Geometry of Polyhedral Distortions: Predictive Relationships for the Phosphate Group. *Acta Crystallographica Section B*, **30**, 1188-1191. https://doi.org/10.1107/S0567740874004560

[61] Tiekink, E.R.T. and Zukerman-Schpector, J. (2012) The Importance of Pi-Interactions in Crystal Engineering: Frontiers in Crystal Engineering. John Wiley & Sons, Ltd., Hoboken, 301-322. https://doi.org/10.1002/9781119945888

[62] Janiak, C. and Chemm, J. (2000) A Critical Account on π-π Stacking in Metal Complexes with Aromatic Nitrogen-Containing Ligands. *Journal of the Chemical Society, Dalton Transactions*, **21**, 3885-3896. https://doi.org/10.1039/b003010o

[63] Banerjee, S., Ghosh, A., Wu, B., *et al.* (2005) Polymethylene Spacer Regulated Structural Divergence in Cadmium Complexes: Unusual Trigonal Prismatic and Severely Distorted Octahedral Coordination. *Polyhedron*, **24**, 593-599. https://doi.org/10.1016/j.poly.2005.01.005

[64] Neve, F., Francescangeli, O. and Crispini, A. (2002) Crystal Architecture and Mesophase Structure of Long-Chain N-Alkylpyridinium Tetrachlorometallates. *Inorganica Chimica Acta*, **338**, 51-58. https://doi.org/10.1016/S0020-1693(02)00976-3

[65] Ertl, A., Hughes, J.M., Pertlik, F., *et al.* (2002) Polyhedron Distortions in Tourmaline. *The Canadian Mineralogist*, **40**, 153-162. https://doi.org/10.2113/gscanmin.40.1.153

[66] Jeffrey, G.A. (1997) An Introduction to Hydrogen Bonding. Oxford University Press, New York.

[67] Spackman, M.A. and Jayatilaka, D. (2009) Hirshfeld Surface Analysis. *CrystEngComm*, **11**, 19-32. https://doi.org/10.1039/B818330A

[68] Panini, P., Mohan, T.P., Gangwar, U., *et al.* (2013) Quantitative Crystal Structure Analysis of 1,3,4-Thiadiazole Derivatives. *CrystEngComm*, **15**, 4549-4564. https://doi.org/10.1039/c3ce40278a

[69] Spackman, M.A. and McKinnon, J.J. (2002) Fingerprinting Intermolecular Interactions in Molecular Crystals. *CrystEngComm*, **4**, 378-392. https://doi.org/10.1039/B203191B

[70] Hirshfeld, F.L. (1977) Bonded-Atom Fragments for Describing Molecular Charge

Densities. *Theoretica Chimica Acta*, **44**, 129-138.
https://doi.org/10.1007/BF00549096

[71] Lassoued, M.S., Abdelbaky, M.S.M., Lassoued, A., *et al.* (2017) Structural Characterization and Physicochemical Features of New Hybrid Compound Containing Chlorate Anions of Cadmate(II). *Journal of Molecular Structure*, **1141**, 390-399.
https://doi.org/10.1016/j.molstruc.2017.03.104

[72] Parkin,, A., Barr, G., Dong, W., *et al.* (2007) Comparing Entire Crystal Structures: Structural Genetic Fingerprinting. *CrystEngComm*, **9**, 648-652.
https://doi.org/10.1039/b704177b

[73] Rohl, A.L., Moret, M., Kaminsky, W., *et al.* (2008) Hirshfeld Surfaces Identify Inadequacies in Computations of Intermolecular Interactions in Crystals: Pentamorphic 1,8-Dihydroxyanthraquinone. *Crystal Growth & Design*, **8**, 4517-4525.
https://doi.org/10.1021/cg8005212

[74] Elwej, R., Hannachi, N., Chaabane, I., *et al.* (2013) Characterization and AC Conductivity of Bis-2-amino-6-picolinium Tetrachloromercurate, $(C_6H_9N_2)_2HgCl_4$. *Inorganica Chimica Acta*, **406**, 10-19. https://doi.org/10.1016/j.ica.2013.06.046

[75] Hannachi, N., Guidara, K., *et al.* (2010) Structural Characterization and AC Conductivity of Bis-Tetrapropylammonium Hexachlorado-Dicadmate, $[N(C_3H_7)_4]_2Cd_2Cl_6$. *Materials Research Bulletin*, **45**, 1754-1761.
https://doi.org/10.1016/j.materresbull.2010.06.035

[76] Wamani, W., Belhouchet, M. and Mhiri, T. (2012) Crystal Structure and Spectroscopic Investigations of a New Benzidinuim Dichloride $NH_3(C_6H_4)_2NH_3Cl_2$. *Materials Science and Engineering*, **28**, Article ID: 012040.
https://doi.org/10.1088/1757-899X/28/1/012040

[77] Mao, W., Wang, J., Liao, H., *et al.* (2019) Crystal Structure and Electrical Conduction of the Organic-Inorganic Compound $(C_6H_9N_2)_2ZnI_4$. *Polyhedron*, **164**, 48-54.
https://doi.org/10.1016/j.poly.2019.02.029

[78] Belhabra, M., Zerraf, S., Kheireddine, A., *et al.* (2018) Structural and Vibrational Study of Diphenylhydrazine Dihydrogenophosphate Single Crystal $(C_6H_9N_2)_2H_2P_2O_7$ (DPHDP). *Chemical Data Collections*, **13**-**14**, 73-83.
https://doi.org/10.1016/j.cdc.2018.01.002

[79] Elwej, R., Hamdi, M., Hannachi, N. and Hlel, F. (2014) Synthesis, Structural Characterization and Dielectric Properties of $(C_6H_9N_2)_2(Hg_{0.75}Cd_{0.25})Cl_4$ Compound. *Spectrochimica Acta*, *Part A*: *Molecular and Biomolecular Spectroscopy*, **121**, 632-640. https://doi.org/10.1016/j.saa.2013.10.109

Supplementary Material

CCDC 1916484 $C_6H_4(NH_3)_2{\cdot}Cl_2$ (**I**) and CCDC 1881531 β-$[C_6H_{10}N_2]_2ZnCl_4$(**II**) contains the supplementary crystallographic data for this paper. The data can be obtained free of charge at https://www.ccdc.cam.ac.uk/structures/? or from the Cambridge Crystallographic Data Center, 12 Union Road, Cambridge CB2 1EZ, UK; fax: 44 1223 336 033; E-mail: deposit@ccda.cam.ac.uk.